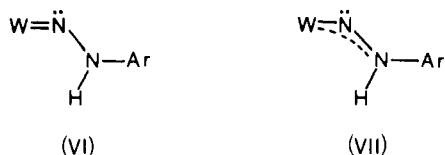


ligands, the structural analysis suggests that, in this complex at least, structure VI makes an important contribution to the overall structure which may be described as VII.



It could indeed be argued that the stability of the bent arylhydrazido(2-) system with regard to the isomeric aryl-diazene may be critically dependent on the ability of the metal to provide a pair of electrons for a metal-nitrogen double bond.

**Reactions of  $\text{CpRe}(\text{CO})_2\text{H}_2$  and  $\text{Cp}_2\text{W}(\text{Ph})\text{H}$ .** As was pointed out previously, the common product of the insertion of an arenediazonium ion into a metal-hydride bond (where such products are stable enough to isolate) is the aryl-diazene complex V (the 1,1-insertion product) rather than the aryl-hydrazido(2-) (or 1,2-insertion product) found for  $\text{Cp}_2\text{WH}_2$ . Therefore, we thought it worthwhile to see what the effect of (i) replacing one hydride ligand or (ii) replacing a Cp ligand by CO would have on the outcome of this reaction. In the first case we used  $\text{Cp}_2\text{W}(\text{Ph})\text{H}$  and, in the second,  $\text{CpRe}(\text{CO})_2\text{H}_2$ . Unfortunately, the changes are drastic enough to completely alter the chemistry.

Addition of an equimolar amount of *p*-fluorobenzenediazonium hexafluorophosphate to  $\text{CpRe}(\text{CO})_2\text{H}_2$  in acetone-hexane at  $-35^\circ\text{C}$  produced no reaction. At room temperature, in acetone-methanol, reaction was complete within 2 days to yield the red complex  $[\text{CpRe}(\text{CO})_2(p\text{-N}_2\text{C}_6\text{H}_4\text{F})][\text{PF}_6]$ , identified by a comparison of its IR spectrum (AgCl cells;  $\nu(\text{CO})$ : 2070, 2010;  $\nu(\text{N}_2)$ : ca.  $1750\text{ cm}^{-1}$ ) and chemical properties (e.g., reaction with KI) with those reported for such complexes previously.<sup>25,26</sup> When the reaction was followed by IR (with AgCl cells), no IR absorptions other than those of either  $\text{CpRe}(\text{CO})_2\text{H}_2$  or the product could be seen, indicating that no intermediate "insertion" product was formed

in an amount detectable in this way. We presume that direct reaction occurs with evolution of hydrogen, but we made no attempt to detect the hydrogen experimentally. The reaction thus appears to parallel the reactions of  $\text{CpRe}(\text{CO})_2\text{HSiPh}_3$  and  $\text{MeCpMn}(\text{CO})_2\text{HSiPh}_3$  in which elimination of  $\text{HSiPh}_3$  occurs and the aryl-diazene complex is formed, without any detectable intermediate insertion product.<sup>26</sup>

The addition of *p*-fluorobenzenediazonium ion to  $\text{Cp}_2\text{W}(\text{Ph})\text{H}$  at  $-30^\circ\text{C}$  in acetone- $d_6$  produced an immediate color change to deep red and evolution of a gas which was presumably nitrogen. An immediate NMR spectrum at  $-30^\circ\text{C}$  showed complete loss of the original resonances of  $\text{Cp}_2\text{W}(\text{Ph})\text{H}$  [ $-11.3$  (H), 4.6 (Cp), 6.6-7.7 ppm (Ph)], together with the formation of a sharp resonance at 7.36 ppm due to benzene and another at 5.6 ppm due to the Cp groups in a product; a multiplet near 7.3 ppm due to the  $\text{FC}_6\text{H}_4$  moiety and/or  $\text{C}_6\text{H}_5$  was also present. Removal of volatiles (consisting largely of acetone- $d_6$  and benzene by GC and NMR) left a red-brown oily residue which could not be successfully purified. A low-nitrogen content (microanalysis) showed it not to be an aryl-diazene or related derivative. Because of this, we have not pursued the reaction further, save to note that upon being warmed to room temperature before evacuation the solution turns deep blue, and evacuation yields a blue solid which we have not investigated. The gas evolution suggests that (i) any aryl-diazene-type intermediate, if formed, rapidly collapses by nitrogen extrusion or (ii) the diazonium ion itself is decomposed by the tungsten compound.

**Acknowledgment.** This work was supported by the Natural Sciences and Engineering Research Council of Canada through operating grants to D. Sutton and F. W. B. Einstein. Professor W. A. G. Graham and Dr. J. K. Hoyano are thanked for a generous gift of  $\text{CpRe}(\text{CO})_2\text{H}_2$  and Professor R. Bau is thanked for communicating a review on metal hydride complexes prior to publication.

**Registry No.**  $[\text{Cp}_2\text{WH}(p\text{-NNC}_6\text{H}_4\text{F})][\text{PF}_6]\cdot\text{Me}_2\text{CO}$ , 76317-79-8.

**Supplementary Material Available:** Table IIIa, a more complete listing of bond lengths and angles, Table V, the torsion angles, Table VI, the mean-plane listing, Table VII, the calculated hydrogen atomic coordinates, Table VIII, a listing of observed and calculated structure amplitudes, and Table IX, the anisotropic thermal parameters (31 pages). Ordering information is given on any current masthead page.

(25) Barrientos-Penna, C. F.; Einstein, F. W. B.; Jones, T.; Sutton, D. *Inorg. Chem.*, companion paper in this issue.

(26) Barrientos-Penna, C. F.; Einstein, F. W. B.; Sutton, D.; Willis, A. C. *Inorg. Chem.* 1980, 19, 2740.

Contribution from the Department of Chemistry,  
The University of North Carolina at Charlotte, Charlotte, North Carolina 28223

## A Novel Series of Compounds Containing from One to Four Ruthenium(II) Bis(bipyridine) Units Bound to the Same Bridging Ligand<sup>1</sup>

D. PAUL RILLEMA,\* ROBERT W. CALLAHAN,\* and KINSLER B. MACK

Received October 15, 1981

The synthesis and properties of a novel series of compounds containing one, two, three, and four ruthenium bis(bipyridine) units bound to the same bridging ligand are described. The formulations were verified by dilution conductivity studies. Both cyclic voltammograms and the visible spectra of the complexes suggest that the bridging ligand can be described as containing two equivalent subunits. The metal centers in the same subunit show the effects of metal-metal interaction in reduction potential data and in the appearance of intervalence electron-transfer bands (IT) for the mixed-valence ions. The metal centers in different subunits act independently of one another. Reduction of the binuclear and tetranuclear complexes results in electronic subunit-subunit interactions at sites closely associated with the pyrazine components.

### Introduction

The behavior of multielectron-transfer agents is an area in inorganic chemistry which has received little attention, pri-

marily for the lack of examples and model compounds. An understanding of the physical properties and reactivity patterns of such complexes is important, especially in light of the fact that multielectron-transfer processes in biochemical reactions are carried out with such ease.<sup>2</sup> Biochemical catalysts may

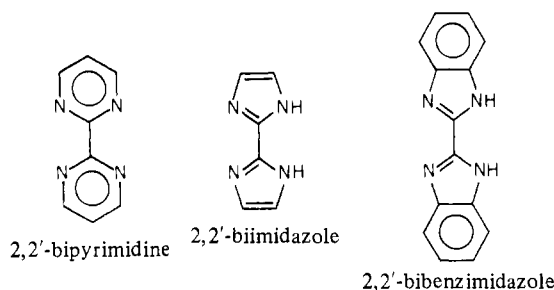
(1) A preliminary account of this work was given at the Southeast/Southwest Regional Meeting of the American Chemical Society, New Orleans, LA, Dec 10-13, 1980.

(2) Griffiths, E. E.; Wharton, D. C. *J. Biol. Chem.* 1961, 236, 1850.

be simple but are more often complex molecules.

Synthetic complexes that duplicate catalytic processes in nature would offer some insight into these. Such catalysts would also be useful in electrochemical applications such as energy conversion, provided the catalysts behaved as photochemical chromophores that were excited by visible light.

One modeling approach in use is to make slight modifications of existing complexes in an attempt to retain their reactivity characteristics. For example, the excited state of  $\text{Ru}(\text{bpy})_3^{2+}$ , where bpy is 2,2'-bipyridine, has been exploited as a one-electron donor or acceptor and various schemes have been devised to use it catalytically for the photochemical preparation of oxygen and hydrogen.<sup>3-11</sup> Slight modifications of the compound by substituting one of the bipyridine ligands by another bidentate ligand such as bipyrimidine,<sup>12,13</sup> biimidazole, or bibenzimidazole<sup>14</sup> have been reported. The

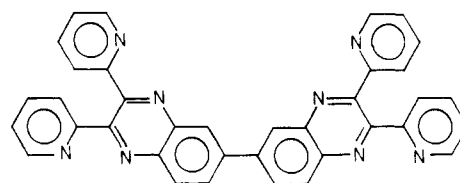


ligands have further been used as bidentate bridging ligands, and both the mononuclear and binuclear species have been isolated. The electrochemical properties of these modified ruthenium complexes suggest that the  $\pi^*$  level of the bipyrimidine ligand lies lower in energy than the  $\pi^*$  level of the bipyridine ligand. For biimidazole complexes, the opposite is true. The potential of the  $\text{Ru}^{\text{III/II}}$  couples also differed. The reduction potentials for the  $\text{Ru}^{\text{III/II}}$  couples of bipyrimidine complexes were  $\sim 0.1$  to  $\sim 0.3$  V greater than those of  $\text{Ru}(\text{bpy})_3^{3+/2+}$ , whereas those for the biimidazole complexes were  $\sim 0.3$  to  $\sim 0.6$  V lower. These observations can be explained on the basis of  $d\pi-\pi^*$  interactions between the  $d\pi$  levels of the ruthenium centers and the lowest lying  $\pi^*$  level of the bridging or bipyridine ligand.<sup>13</sup>

The mononuclear complexes containing the bipyrimidine and biimidazole bridging ligands were reported to luminesce similarly to  $\text{Ru}(\text{bpy})_3^{2+}$ , although quantum yields were not given. Binuclear complexes, however, were found to be nonemitters.<sup>12-14</sup> Oxidation of  $[\text{Ru}(\text{bpy})_2(\text{BL})]^{4+}$  to  $[\text{Ru}(\text{bpy})_2(\text{BL})]^{5+}$ , where BL represents a bidentate bridging ligand, resulted in formation of a mixed-valence complex. A near-infrared absorption band for the bibenzimidazole complex was observed at  $5.3 \times 10^3 \text{ cm}^{-1}$ . The band contained features

similar to those of intervalence electron transfer (IT) found for metal-bridged complexes containing weak metal-metal interactions.<sup>15</sup> Such interactions provide a pathway for facile electron exchange in binuclear complexes. The rate of thermal exchange ( $k_{\text{et}}$ ) between metal centers was calculated to be  $\sim 10^9 \text{ s}^{-1}$  for  $[\text{Cl}(\text{phen})_2\text{Ru}]_2\text{pyr}^{5+}$ , where phen is *o*-phenanthroline and pyr is pyrazine, and substituted phenanthroline complexes.<sup>16,17</sup> Thus, multielectron transfer to a substrate associated with one metal site is possible in binuclear complexes of this type.

We not only have extended investigations to include binuclear complexes with bidentate ligands like bipyridine, biimidazole, and bibenzimidazole but also have prepared a series of complexes using the bridging ligand



2,2',3,3'-tetra-2-pyridyl-6,6'-biquinoxaline (BL)

It contains four bidentate sites for chelating to metal centers. Each successive site has been complexed to a ruthenium center, and the compounds have been isolated and characterized. This paper describes these unique compounds.

### Experimental Section

**Materials.** Tetra-*n*-butylammonium hexafluorophosphate (TBAH) was prepared by standard techniques,<sup>18</sup> recrystallized three times from hot ethanol-water mixtures, and vacuum dried at 70 °C for 10 h. Tetraethylammonium perchlorate (TEAP) was purchased as reagent grade, recrystallized three times from distilled water followed by a final recrystallization from a 1:1 methanol-acetone solution, and then dried under vacuum overnight. Acetonitrile was either spectral or pesticide grade and was dried 48 h over 4-Å molecular sieves before use. Nitrogen was scrubbed by passing it through a solution  $\sim 2.4$  M in hydrochloric acid and  $\sim 0.4$  M in chromous chloride generated from chromic chloride over zinc-mercury amalgam. Elemental analyses were carried out by Integral Laboratories, Inc., Raleigh, NC.

**Preparations.** The preparations of the salts  $\text{Ru}(\text{bpy})_3(\text{PF}_6)_2$ <sup>19</sup> and  $\text{Ru}(\text{bpy})_2\text{Cl}_2 \cdot 2\text{H}_2\text{O}$ <sup>20</sup> were described previously.

**Bridging Ligand, BL.** Both 3,3'-diaminobenzidine (1.0 g, 4.67 mmol) and 2,2'-pyridyl (2.0 g, 9.34 mmol) were added to a 100 mL flask. Then 50 mL of anhydrous ethanol was added, and the mixture was stirred and heated under reflux for 1 h, during which time a yellow precipitate formed. The product was filtered, washed with small portions of cold ethanol followed by ether, and air-dried. Anal. Calcd for  $\text{C}_{36}\text{H}_{22}\text{N}_8$ : C, 76.3; H, 3.9; N, 19.8. Found: C, 76.3; H, 3.3; N, 19.3.

**$[\text{Ru}(\text{bpy})_2\text{BL}(\text{PF}_6)_2]$ .** The mononuclear complex was prepared by adding 2.14 mmol of BL to 80 mL of a 1:1 water-methanol solution, dissolving the ligand by the dropwise addition of 6 M HCl until soluble, and then refluxing the resulting solution for 4 h in the presence of 0.536 mmol of  $\text{Ru}(\text{bpy})_2\text{Cl}_2 \cdot 2\text{H}_2\text{O}$ . The solution became red during the refluxing period. Excess ligand was then precipitated by neutralization of the HCl with 6 M NaOH. Finally the mononuclear complex was precipitated as the hexafluorophosphate salt by addition of a saturated, aqueous  $\text{NH}_4\text{PF}_6$  solution. The compound was collected by filtration, then dissolved in acetone, and chromatographed on a neutral alumina column developed with acetone. The first fraction

- (3) For recent reviews see: (a) Whitten, D. G. *Acc. Chem. Res.* **1980**, *13*, 83. (b) Sutin, N.; Creutz, C. *Adv. Chem. Ser.* **1978**, *No. 168*, 1.
- (4) Kalyanasundaram, K.; Kiwi, J.; Gratzel, M. *Helv. Chim. Acta* **1978**, *61*, 2720.
- (5) Durham, B.; Dressick, W. J.; Meyer, T. J. *J. Chem. Soc., Chem. Commun.* **1979**, 381.
- (6) DeLaive, P. J.; Sullivan, B. P.; Meyer, T. J.; Whitten, D. G. *J. Am. Chem. Soc.* **1979**, *101*, 4007.
- (7) Kirch, M.; Lehn, J. M.; Sauvage, J. P. *Helv. Chim. Acta* **1979**, *62*, 1345.
- (8) Brown, G. M.; Chan, S. F.; Creutz, C.; Schwarz, H. A.; Sutin, N. *J. Am. Chem. Soc.* **1979**, *101*, 7638. Brown, G. M.; Brunschwig, B. S.; Creutz, C.; Endicott, J. F.; Suttin, N. *Ibid.* **1979**, *101*, 1298.
- (9) Ziessel, R.; Lehn, J. M.; Sauvage, J. P. *Nouv. J. Chem.* **1979**, *3*, 423.
- (10) Rillema, D. P.; Dressick, W. J.; Meyer, T. J. *J. Chem. Soc., Chem. Commun.* **1980**, 247. Kobayashi, C. O.; Furuta, N.; Shimura, O. *Chem. Lett.* **1976**, 503.
- (11) Kiwi, J.; Gratzel, M. *J. Am. Chem. Soc.* **1979**, *101*, 7214. Kalyanasundaram, K.; Gratzel, M. *Angew. Chem., Int. Ed. Engl.* **1979**, *18*, 701.
- (12) Hunziker, M.; Ludi, A. *J. Am. Chem. Soc.* **1977**, *99*, 7370.
- (13) Dose, E. V.; Wilson, L. *Inorg. Chem.* **1978**, *17*, 2660.
- (14) Haga, M.-A. *Inorg. Chim. Acta* **1980**, *45*, L183.

- (15) Meyer, T. J. *Acc. Chem. Res.* **1978**, *11*, 94 and references therein.
- (16) Cloninger, K. K.; Callahan, R. W. *Inorg. Chem.* **1981**, *20*, 1611.
- (17) Lin, C. T.; Botcher, W.; Chou, M.; Creutz, C.; Sutin, N. *J. Am. Chem. Soc.* **1976**, *98*, 6536.
- (18) Sawyer, D. T.; Roberto, J. L. "Experimental Electrochemistry for Chemists"; Wiley: New York, 1974.
- (19) Braddock, J. N.; Meyer, T. J. *J. Am. Chem. Soc.* **1973**, *95*, 3158.
- (20) Sprintschnik, G.; Sprintschnik, H. W.; Kirsch, P. O.; Whitten, D. G. *J. Am. Chem. Soc.* **1976**, *98*, 2337.

was eluted with a 1:1 acetone–methylene chloride solution, and it contained a small amount of a yellow-orange impurity. The emission spectrum of this fraction was similar to that of  $\text{Ru}(\text{bpy})_3^{2+}$ , which perhaps was formed from the original  $\text{Ru}(\text{bpy})_2\text{Cl}_2$  starting material via rearrangement during the preparation. The column was further eluted with acetone until the red band moved down the column. The red band was then eluted from the column with acetonitrile. The middle fraction was collected, concentrated to about 30 mL, and then added to ether to precipitate the compound. The solid was suction filtered, washed with ether, and then air-dried. Anal. Calcd for  $[\text{Ru}(\text{bpy})_2]\text{BL}(\text{PF}_6)_2$ : C, 53.0; H, 3.0; N, 13.2. Found: C, 52.7; H, 3.0; N, 13.1.

**$[\text{Ru}(\text{bpy})_2]_2\text{BL}(\text{PF}_6)_4$  and  $[\text{Ru}(\text{bpy})_2]_3\text{BL}(\text{PF}_6)_6 \cdot 6\text{H}_2\text{O}$ .**  $\text{Ru}(\text{bpy})_2\text{Cl}_2 \cdot 2\text{H}_2\text{O}$  (1.00 g, 1.92 mmol) was suspended in deaerated acetone (~200 mL), and  $\text{AgPF}_6$  (0.971 g, 3.84 mmol) was added. The resulting suspension was stirred under  $\text{N}_2$  and heated to nearly boiling for ~3 h. The solution of  $\text{Ru}(\text{bpy})_2\text{S}_2^{2+}$ , S = acetone, was filtered under  $\text{N}_2$  to remove  $\text{AgCl}$ . Then BL (1.09 g, 1.92 mmol) was added to the filtrate, and the resulting suspension was refluxed under  $\text{N}_2$  for 24 h. It was found that the shorter reflux times (4 h) favored formation of the binuclear complex; longer times favored formation of the trinuclear species. The unreacted bridging ligand was then removed by filtration. The filtrate was then concentrated to approximately 30 mL and added to ether to precipitate the compounds. The solid was collected by filtration, redissolved in acetone, and then chromatographed on a neutral alumina column developed with acetone. As found above in the preparation of the mononuclear species, initial elution of the column with a 1:1 acetone–methylene chloride solution resulted in separation of a yellow compound having emission properties similar to those of  $\text{Ru}(\text{bpy})_3^{2+}$ . The fraction was discarded, and acetone was used to move the subsequent red band. The band was then eluted with a 1:1 acetone–acetonitrile solution. The middle fraction was collected and concentrated to ~30 mL, and the binuclear complex was precipitated by addition to ether. Anal. Calcd for  $[\text{Ru}(\text{bpy})_2]_2\text{BL}(\text{PF}_6)_4$ : C, 46.3; H, 2.8; N, 11.4. Found: C, 46.1; H, 2.5; N, 11.2.

A green band characteristic of the trinuclear complex remained on the column after the remaining binuclear complex was eluted from the column with acetonitrile. The green band was removed from the column by eluting with a 1:1 methanol–acetonitrile solution. The eluant was concentrated and added to ether to precipitate the trinuclear complex. It was suction filtered, washed with ether, and air-dried. Anal. Calcd for  $[\text{Ru}(\text{bpy})_2]_3\text{BL}(\text{PF}_6)_6 \cdot 6\text{H}_2\text{O}$ : C, 41.4; H, 3.0; N, 10.1. Found: C, 41.6; H, 2.7; N, 10.0.

**$[\text{Ru}(\text{bpy})_2]_4\text{BL}(\text{PF}_6)_8 \cdot 8\text{H}_2\text{O}$ .**  $\text{Ru}(\text{bpy})_2\text{Cl}_2 \cdot 2\text{H}_2\text{O}$  (0.316 g, 0.61 mmol) was suspended in deaerated acetone (~25 mL), and  $\text{AgPF}_6$  (0.308 g, 1.22 mmol) was added. After ~3 h of stirring at room temperature under  $\text{N}_2$ , the red solution of  $\text{Ru}(\text{bpy})_2\text{S}_2^{2+}$ , S = acetone, was filtered to remove  $\text{AgCl}$ .  $[\text{Ru}(\text{bpy})_2]_2\text{BL}(\text{PF}_6)_4$  (0.600 g, 0.30 mmol) was added to the filtrate, and the solution was refluxed under  $\text{N}_2$  for ~24 h. After the solution cooled, ethanol was slowly added until cloudiness developed. After ~48 h, the crude green product was collected. A second purification from acetone–ethanol gave the pure product, which was collected, washed with ethanol, and dried under vacuum. Anal. Calcd for  $[\text{Ru}(\text{bpy})_2]_4\text{BL}(\text{PF}_6)_8 \cdot 8\text{H}_2\text{O}$ : C, 39.5; H, 2.9; N, 9.5. Found: C, 39.7; H, 2.5; N, 9.5.

**Physical Measurements.** Infrared spectra of the compounds were recorded in Nujol mulls with a Perkin-Elmer 457 spectrophotometer. Near-infrared, visible, and UV spectra were recorded with the Cary 14 or 17 instrument. Solution conductivities were obtained in acetonitrile at  $25.0 \pm 0.1$  °C with a Model RC-18A Beckman conductivity bridge. The temperature of the solution was controlled with a Haake FK-2 constant-temperature bath. Polarograms were obtained in 0.1 M TEAP–acetonitrile solutions with a PAR 174 polarographic analyzer or the PAR 173 potentiostat in conjunction with the PAR 174 programmer. Polarograms were recorded with a Houston Omni-graphic X-Y recorder. Coulometry was performed with the PAR 173 potentiostat, the PAR 179 digital coulometer, and the PAR 370 cell system. Luminescence spectra were determined in acetonitrile solutions with a Perkin-Elmer 650-40 instrument. The spectra were uncorrected for instrument response. Both entrance and exit slits were open to their maximum (20 nm) due to the weak luminescence of the products.

## Results

**Preparations.** The preparations described in the Experimental Section utilized the synthetic intermediate Ru-

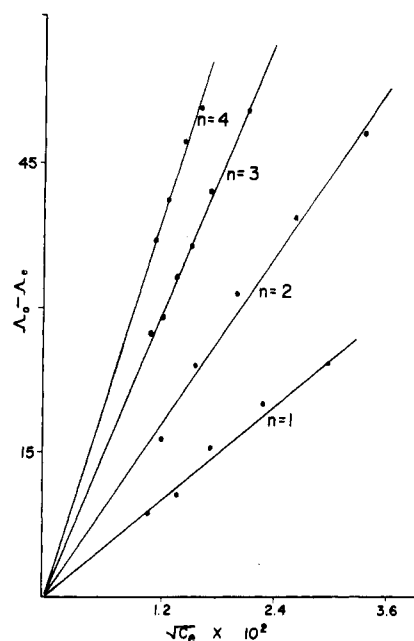


Figure 1. Dilution conductivities of  $[\text{Ru}(\text{bpy})_2]_n\text{BL}(\text{PF}_6)_{2n}$  in acetonitrile at 25 °C.  $n = 1-4$ .

$(\text{bpy})_2\text{S}_2^{2+}$ , S = solvent, generated by removal of bound chloride from  $\text{Ru}(\text{bpy})_2\text{Cl}_2$  after addition of  $\text{AgPF}_6$  to a suspension of  $\text{Ru}(\text{bpy})_2\text{Cl}_2$  in acetone or simply refluxing  $\text{Ru}(\text{bpy})_2\text{Cl}_2$  in water. The desired complexes were formed by substitution of one of the bidentate chelating sites of the bridging ligand for weakly coordinated solvent. Similar procedures have been reported for the preparation of bipyrimidine,<sup>12,13</sup> biimidazole,<sup>13</sup> and bibenzimidazole<sup>14</sup> complexes of  $\text{Ru}(\text{bpy})_2\text{S}_2^{2+}$ . The binuclear complex formed preferentially upon addition of the bridging ligand to a solution containing  $\text{Ru}(\text{bpy})_2\text{S}_2^{2+}$  in acetone. Formation of the mononuclear complex required blockage of the basic nitrogen sites of the bridging ligand with  $\text{H}^+$ . Formation of the trinuclear and tetranuclear species required reflux conditions in acetone longer than needed to prepare the binuclear species.

As shown by infrared and elemental analyses, some of the salts reported contain waters of crystallization, which are held tenaciously. Strong association of molecules of water with other  $\alpha, \alpha$ -diimine complexes has been noted previously.<sup>21-24</sup>

**Conductivity.** Dilution conductivities were determined for the complexes in acetonitrile. According to eq 1, the equivalent

$$\Delta_c = \Delta_0 - AC_{\text{eq}}^{1/2} \quad (1)$$

conductance,  $\Delta_c$ , varies linearly with the square root of the equivalent concentration.<sup>25</sup> For strong electrolytes, plots of  $\Delta_c$  vs.  $C_{\text{eq}}^{1/2}$  should be linear and the intercept represents the equivalent conductance at infinite dilution,  $\Delta_0$ . Experimentally, it has been shown that the slope depends on the type of electrolyte.<sup>26,27</sup> The utility of the method then allows discrimination between various charge types formed upon ionization of the compounds in solution and provides experimental

- (21) Gere, D. R.; Meloan, C. E. *J. Inorg. Nucl. Chem.* **1963**, *25*, 1507.
- (22) Burchett, S.; Meloan, C. E. *J. Inorg. Nucl. Chem.* **1972**, *34*, 1207.
- (23) LaMar, G. N.; Van Hecke, G. R. *Inorg. Chem.* **1973**, *12*, 1767.
- (24) Callahan, R. W.; Brown, G. M.; Meyer, T. J. *Inorg. Chem.* **1975**, *14*, 1443.
- (25) Boggess, R. K.; Zatzko, D. A. *J. Chem. Educ.* **1975**, *52*, 649 and references therein.
- (26) Feltham, R. D.; Hayter, R. G. *J. Chem. Soc.* **1964**, 4587.
- (27) Weaver, T. R.; Meyer, T. J.; Adeyemi, S. A.; Brown, G. M.; Eckberg, R. P.; Hatfield, W. E.; Johnson, E. C.; Murray, R. W.; Untereker, D. *J. Am. Chem. Soc.* **1975**, *97*, 3039.

Table I. Electrochemical Data for  $[\text{Ru}(\text{bpy})_2]_n\text{BL}^{2n+}$  ( $n = 1-4$ )

| complex                                     | oxidations         |                    |                     | reductions |                     |                   |                     |                     |
|---|--------------------|--------------------|---------------------|------------|---------------------|-------------------|---------------------|---------------------|
|   | $E_{1/2}(2)^{a,b}$ | $E_{1/2}(1)^{a,b}$ | $E_{1/2}(1')^{a,b}$ | $n^c$      | $E_{1/2}(2')^{a,b}$ | $n^c$             | $E_{1/2}(3')^{a,b}$ | $E_{1/2}(4')^{a,b}$ |
| $[\text{Ru}(\text{bpy})_2]\text{BL}^{2+}$   |                    | 1.41 (61)          | -0.72 (69)          | 1.06       |                     |                   | -1.41 (70)          |                     |
| $[\text{Ru}(\text{bpy})_2]_2\text{BL}^{4+}$ |                    | 1.42 (61)          | -0.67 (60)          |            | -0.80 (60)          | 1.98 <sup>d</sup> | -1.41 <sup>c</sup>  |                     |
| $[\text{Ru}(\text{bpy})_2]_3\text{BL}^{6+}$ | 1.63 (68)          | 1.46 (58)          | -0.31 (75)          | 0.95       | -0.72 (80)          | 1.00              | -1.10 (85)          |                     |
| $[\text{Ru}(\text{bpy})_2]_4\text{BL}^{8+}$ | 1.64 (69)          | 1.46 (64)          | -0.22 (65)          |            | -0.36 (55)          | 2.00 <sup>d</sup> | -1.01 (60)          | -1.17 (54)          |

<sup>a</sup> Potential measurements were at a Pt electrode and referred to a saturated sodium calomel electrode (SSCE) in 0.1 M TEAP-CH<sub>3</sub>CN at 20 ± 1 °C. The estimated error is ±0.01 V. <sup>b</sup>  $\Delta E_p$  values are given in parentheses and were extrapolated from the intercepts of plots of  $\Delta E_p$  vs.  $v^{1/2}$ , where  $v$  is the sweep rate. <sup>c</sup> Error of coulometric  $n$  values is ±0.05. <sup>d</sup>  $n$  value corresponds to the sum of  $E_{1/2}(1') + E_{1/2}(2')$ .

support for the formulations of the compounds proposed from elemental analyses.

Equivalent conductivities were determined by the formula

$$\Lambda_e = \left( \frac{1}{R} - \frac{1}{R_s} \right) \frac{1000k}{C_{\text{eq}}} \quad (2)$$

where  $R$  is the solution resistance,  $R_s$  is the resistance of the pure solvent, and  $k$  is the cell constant. Plots of  $\Lambda_e$  vs.  $C_{\text{eq}}^{1/2}$  for the complexes were linear as expected. Values of  $\Lambda_0$  were used to construct plots of  $\Lambda_0 - \Lambda_e$  vs.  $C_{\text{eq}}^{1/2}$  shown in Figure 1. The slopes of the lines were determined by a linear least-squares regression analysis and compared favorably to the theoretical slopes determined from the Onsager equation<sup>25</sup>

$$\Lambda_e = \Lambda_0 - \left[ \frac{41.25}{\eta(\epsilon T)^{1/2}} (|z^+| + |z^-|) + \frac{2.801 \times 10^6}{(\epsilon T)^{3/2}} \frac{q}{1 + q^{1/2}} |z^+ z^-| \Lambda_0 \right] l^{1/2} \quad (3)$$

where

$$q = \frac{|z^+ z^-|}{|z^+| + |z^-|} \frac{\lambda_+^\circ + \lambda_-^\circ}{|z^-| \lambda_+^\circ + |z^+| \lambda_-^\circ}$$

and

$$I = \frac{C_{\text{eq}}}{2} (n_+ z_+^2 + n_- z_-^2)$$

and  $n_+$  and  $n_-$  are used to convert  $C_m$  to  $C_{\text{eq}}$  from the usual ionic strength equation

$$I = \frac{1}{2} \sum_i C_{m_i} z_i^2$$

In eq 3,  $\epsilon$  = dielectric constant of the solvent (36.0 for acetonitrile),  $\eta$  = the viscosity of the solvent in poise (3.448 P for acetonitrile),  $T$  is the absolute temperature,  $z_i$  is the charge of the ion, and  $\lambda_i^\circ$  is the limiting conductivity of each ion at infinite dilution. The  $\lambda_-^\circ$  value used for  $\text{PF}_6^-$  was 102.9.<sup>25</sup> The Kohlraush equation,  $\Lambda_0 = \lambda_+^\circ + \lambda_-^\circ$ , was used to calculate  $\lambda_+^\circ$ .

The experimental slopes from the mononuclear to the tetranuclear complex were  $701 \pm 48$ ,  $1541 \pm 93$ ,  $2494 \pm 80$ , and  $3296 \pm 136$  mhos·L<sup>1/2</sup>·equiv<sup>-1/2</sup>, respectively; the theoretical values were 822, 1543, 2464, and 3263 mhos·L<sup>1/2</sup>·equiv<sup>-1/2</sup>, in the same order. Standards were also run for direct comparison purposes. The experimental slopes for  $\text{Ru}(\text{bpy})_3(\text{PF}_6)_2$ , a 2:1 electrolyte, was  $826 \pm 24$  mhos·L<sup>1/2</sup>·equiv<sup>-1/2</sup> and that of TBAH, a 1:1 electrolyte, was  $208 \pm 25$  mhos·L<sup>1/2</sup>·equiv<sup>-1/2</sup>.

The conductivity results verify the formulations of the compounds as 2:1, 4:1, 6:1, and 8:1 electrolytes. To our knowledge, this is the first series to be so clearly defined.

**Electrochemistry.** Cyclic voltammograms for the compounds are illustrated in Figures 2 and 3, and important electrochemical data are given in Table I. Peak potentials were scan rate dependent. Plots of  $\Delta E_p$ , where  $\Delta E_p = E_{\text{ox}} -$

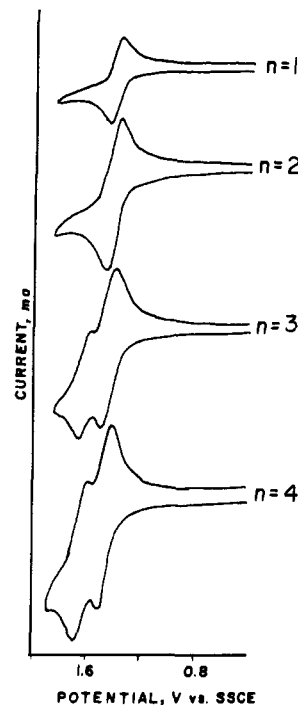


Figure 2. Cyclic voltammograms for  $[\text{Ru}(\text{bpy})_2]_n\text{BL}^{2n+}$  oxidations in acetonitrile solutions containing 0.1 M TEAP as supporting electrolyte.  $T = 20 \pm 1$  °C.  $n = 1-4$ . Concentrations of complexes were  $5 \times 10^{-4}$  M.

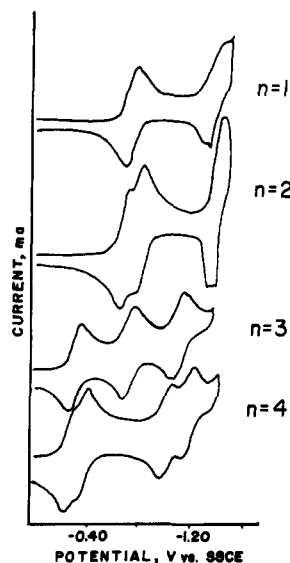


Figure 3. Cyclic voltammograms for successive reductions of  $[\text{Ru}(\text{bpy})_2]_n\text{BL}^{2n+}$  in acetonitrile containing 0.1 M TEAP as supporting electrolyte.  $T = 20 \pm 1$  °C.  $n = 1-4$ . Concentrations of complexes were  $5 \times 10^{-4}$  M.

$E_{\text{red}}$ , vs. the square root of the sweep rate were linear, indicating that the electron-transfer processes were reversible.<sup>28</sup> The

Table II. Spectral Data for  $[\text{Ru}(\text{bpy})_2]_n\text{BL}(\text{PF}_6)_2n^a$ 

|   |                            |                            |                            |                            |                            |
|---|----------------------------|----------------------------|----------------------------|----------------------------|----------------------------|
| $[\text{Ru}(\text{bpy})_2]_1\text{BL}^{2+}$ | 525 ( $8.49 \times 10^3$ ) | 420 (sh)                   | 381 ( $3.24 \times 10^4$ ) | 284 ( $9.50 \times 10^4$ ) | 244 ( $5.70 \times 10^4$ ) |
| $[\text{Ru}(\text{bpy})_2]_2\text{BL}^{4+}$ | 528 ( $1.63 \times 10^4$ ) | 410 ( $4.49 \times 10^4$ ) | 362 (sh)                   | 284 ( $1.54 \times 10^5$ ) | 244 ( $6.68 \times 10^4$ ) |
| $[\text{Ru}(\text{bpy})_2]_3\text{BL}^{6+}$ | 616 ( $2.06 \times 10^4$ ) | 542 ( $1.74 \times 10^4$ ) | 424 ( $6.12 \times 10^4$ ) | 278 ( $1.23 \times 10^5$ ) |                            |
| $[\text{Ru}(\text{bpy})_2]_4\text{BL}^{8+}$ | 622 ( $3.40 \times 10^4$ ) |                            | 425 ( $7.01 \times 10^4$ ) | 285 ( $5.50 \times 10^5$ ) |                            |

<sup>a</sup>  $\lambda_{\text{max}}$  is in nm; error  $\pm 1$  nm.  $\epsilon$  values follow in parentheses.  $\epsilon$  values are in units  $\text{M}^{-1} \text{cm}^{-1}$ ; error  $\pm 5\%$ . Spectra are recorded for solutions in acetonitrile at  $20 \pm 1$  °C.

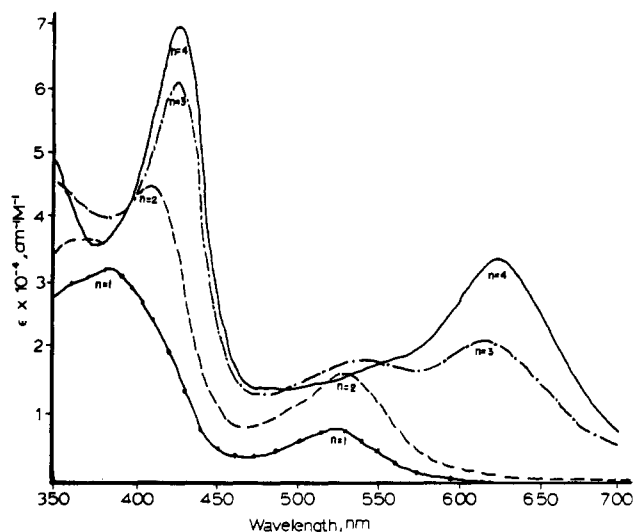


Figure 4. Visible spectra of  $[\text{Ru}(\text{bpy})_2]_n\text{BL}^{2n+}$  in acetonitrile at  $20 \pm 1$  °C:  $n = 1$  (—•—•—);  $n = 2$  (---);  $n = 3$  (-·-·-·-);  $n = 4$  (—).

sweep rate was varied from 800 to 20 mV/s, and  $\Delta E_p$  varied from 70 to 60 mV. Limiting values of the peak potential separations were extrapolated from the plots and are recorded in Table I.

In a large number of cases the values were only slightly larger than the theoretical value required for a one-electron-transfer process.<sup>28</sup> Cases where there were generally exceptions resulted from situations where redox processes were insufficiently separated from one another and areas under the waves were added together, causing  $\Delta E_p$  to be larger for the more anodic voltammogram. *iR* compensation was used in an effort to correct the problem, but little difference was noted between experiments with or without use of this feature.

The only electrochemical processes readily characterized by coulometry were the first reduction of the mononuclear species, the first and second reductions for the trinuclear complex, and the combination of the first and second reductions of the binuclear and tetranuclear compounds. The  $n$  values are listed in Table I. Coulometric reductions of the more negative redox processes were complicated by electrode absorption problems and insufficient separation of that reduction from another at slightly more negative potential. The second reduction wave of the binuclear complex ( $n = 2$ ) in Figure 3 illustrates these problems. Coulometric oxidations were complicated by rearrangement of the starting material as noted by the appearance of a new cyclic wave at more positive potential than the original wave and catalysis as indicated by the inability of the coulometric recorder trace to reach the expected base line. The oxidation processes are currently being explored in our laboratories.<sup>29</sup>

**Visible-Ultraviolet Spectra.** The visible spectra of the four compounds are shown in Figure 4. A summary of the important visible-ultraviolet features is given in Table II. The absorption coefficients were obtained from Beer's law studies

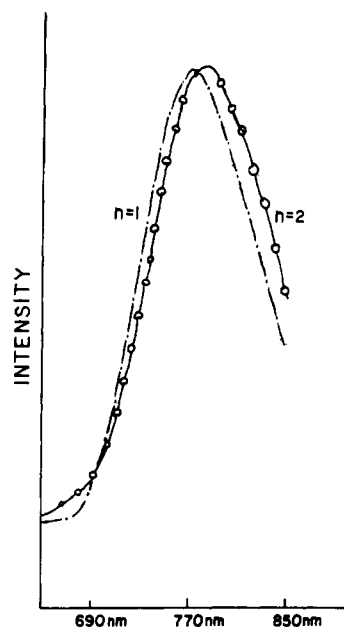


Figure 5. Emission spectra of  $[\text{Ru}(\text{bpy})_2]_n\text{BL}^{2n+}$  in acetonitrile at  $20 \pm 1$  °C:  $n = 1$  (-·-·-·-);  $n = 2$  (-O-). Spectra are uncorrected.

and were determined from at least four dilution points. The probable assignments for the absorption bands based on an analysis of the absorption spectrum of  $\text{Ru}(\text{bpy})_3^{2+}$ <sup>30</sup> will be discussed in a latter section.

**Luminescence Spectra.** Luminescence spectra were obtained for the mononuclear and binuclear complexes and are illustrated in Figure 5. There is only about a 10-nm separation between the two peak positions with the maximum of the binuclear complex shifted slightly more to the red. The spectra are uncorrected for instrumental factors and solution self-absorption. The two compounds are weak emitters with  $\Phi \approx (6 \pm 1) \times 10^{-6}$ . The method of Guilbault was used for the quantum yield determinations.<sup>31</sup> These were deduced by comparison to  $\text{Ru}(\text{bpy})_3^{2+}$  having a known quantum yield of 0.04 at  $\lambda_{\text{ex}} = 436$  nm.<sup>32</sup> Excited-state lifetimes were extremely short and estimated to be  $\leq 60$  ns.<sup>33</sup> No luminescence was observed for the trinuclear or tetranuclear species.

## Discussion

**Compound Formulation.** The bridging ligand BL has four bidentate sites, each with potential for chelation. The substitution pattern of complexing  $\text{Ru}(\text{bpy})_2^{2+}$  units could involve the coordination of a second metal to the same pyrazine residue as the first, or the species could bind to the uncomplexed one

(28) Nicholson, R. S.; Shain, I. *Anal. Chem.* **1964**, *36*, 705.

(29) A preliminary account of our results was given at the Conference on Inorganic Reaction Mechanisms, Wayne State University, Detroit, MI, June 10-12, 1981.

(30) Bryant, G. M.; Ferguson, J. E.; Powell, H. K. *Aust. J. Chem.* **1971**, *24*, 275. Lytle, F. E.; Hercules, D. M. *J. Am. Chem. Soc.* **1969**, *91*, 253.

(31) Guilbault, G. "Practical Fluorescence, Theory, Methods and Techniques"; Marcel Dekker: New York, 1973; pp 11-14.

(32) Sullivan, B. P.; Salmon, D. J.; Meyer, T. J.; Peedin, J. *Inorg. Chem.* **1979**, *18*, 336 and references therein.

(33) Excited-state lifetimes were measured at The University of North Carolina at Chapel Hill by using a laser flash photolysis spectrophotometer described previously.<sup>34</sup>

(34) Bock, C. R. Ph.D. Dissertation, The University of North Carolina, 1974. Young, R. C. Ph.D. Dissertation, The University of North Carolina, 1976. Nagle, J. K. Ph.D. Dissertation, The University of North Carolina, 1979.

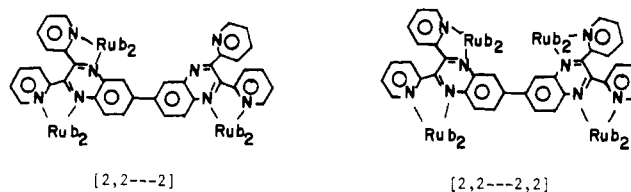
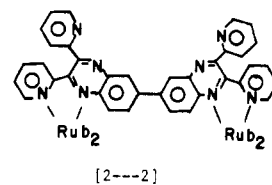
more distant. Spectral and electrochemical data indicate that the latter is the case. According to Figure 4, the position of the first absorption maximum ( $\sim 525$  nm) remains nearly constant but  $\epsilon$  doubles upon complexation of the second  $\text{Ru}(\text{bpy})_2^{2+}$  component. Another peak at lower energy is found to "grow in" upon addition of the third  $\text{Ru}(\text{bpy})_2^{2+}$  unit to the bridging ligand, consistent with what is observed in cases where metal-metal interaction occurs.<sup>12,13,24</sup> This interaction has been ascribed to a combination of charge and electronic factors, although the electrostatic component is dominant.<sup>24</sup> This effect lowers the level of the  $\pi^*$  ligand orbitals and, hence, the energy of the first transition. Finally, upon filling of the remaining site, the low-energy band increases in intensity at the expense of the original absorption near 525 nm.

Electrochemical oxidations shown in Figure 2 can be explained in a similar way. The voltammograms were obtained at equimolar concentrations for direct comparisons. The first oxidations of  $\text{Ru}(\text{bpy})_3^{2+}$  and substituted analogues  $\text{Ru}(\text{bpy})_2\text{L}_2^{n+}$  or  $\text{Ru}(\text{bpy})_2\text{XL}^+$ , where L is a monodentate ligand and X is a halide ion, have been reported to involve the  $\text{Ru}^{\text{III/II}}$  couple,<sup>16,24,35,36</sup> and thus, a similar explanation would apply here also. Within experimental error, the half-wave potentials for the first oxidation of the mononuclear and binuclear complexes are similar. However, the area under the voltammogram of the binuclear complex is twice that of the mononuclear species and corresponds to two one-electron-transfer processes. There is no evidence for peak "splitting" even though statistical factors require at least a 36-mV spacing between the two oxidation waves.<sup>37</sup> In addition, the peak heights are in a ratio of 1:1.8 consistent with the fact pointed out by Taube<sup>38</sup> that there is no theoretical basis for expecting the ratio of peak currents for a two one-electron to one one-electron process to be 1:2.

Addition of the third ruthenium center to the bridging ligand results in the appearance of another wave in a manner similar to that observed for interaction between two metal centers. The origin of this effect was discussed above in regard to the absorption spectra of the compounds. For metal oxidations, the effect removes the degeneracy of the  $d\pi$  orbitals on the metal centers after the first electron is removed, resulting in a second wave at a potential slightly more positive than the first. This second oxidation wave increases in magnitude upon addition of the fourth  $\text{Ru}(\text{bpy})_2^{2+}$  unit to the bridging ligand, becoming a two one-electron wave similar to the first wave.

The conclusion is the binuclear complex is best represented as  $[2---2]$ , the trinuclear complex as  $[2,2---2]$ , and the tetranuclear complex as  $[2,2---2,2]$ , where the dashed line acknowledges the fact that the metal centers are held together by a bridging ligand but the interaction between the metal centers is at best very weak (see structures). Essentially then, according to the way the metal centers behave, the bridging ligand can be described as containing two bridging ligand subunits held together by the bond between the two benzene rings.

**Reduction Processes.** The reduction processes for the compounds are illustrated in Figure 3. Reduction of the mononuclear complex results in the appearance of two waves. The first at  $-0.82$  V vs. SSCE having an  $n$  value of 1.06 is assigned to reduction of the bridging ligand; the second wave at  $-1.41$  V most likely corresponds to reduction of the bipyridine ligand.<sup>40</sup> Reduction of  $[2---2]$  results in "splitting"



of the first wave of the monomer into two waves separated by 130 mV. The waves were too close to obtain an  $n$  value for each; the composite, however, was 1.98, indicating that each is a one-electron process. The wave "splitting" is similar to that found for metal-metal interacting sites and strongly suggests that the two reductions occur at equivalent positions on each bridging ligand subunit closely associated with the metal centers (probably the pyrazine moiety) and the reduced sites sense each other's presence by charge interaction.

Three reduction waves are observed in Figure 3 for the trinuclear complex. The outer two result from the  $([2,2---])$  component, and the inner one results from the mononuclear part  $(---2]$  superimposed. DeArmond<sup>40</sup> has shown that reductions of bipyridine ligands bound to the same metal center occur stepwise in a series followed by a second reduction series approximately 0.6–0.7 V more negative than the first. The addition of the third  $\text{Ru}(\text{bpy})_2^{2+}$  unit to form the  $([2,2---])$  component shifts the first reduction wave from  $-0.72$  to  $-0.31$  V vs. SSCE. According to DeArmond,<sup>40</sup> the second reduction of that site would be located approximately at  $-1.0$  V vs. SSCE. The reduction at  $-1.10$  V vs. SSCE would correlate well with the second reduction of that bridging ligand subunit. Since the  $\pi^*$  levels of the  $([2,2---])$  and  $(---2]$  components are not equivalent, the reductions seem to occur independently of one another. In fact, the reduction of the  $(---2]$  portion occurs at the position expected for the mononuclear species. The reductions at  $-0.31$  V vs. SSCE and  $-0.72$  V vs. SSCE are both one-electron processes having  $n$  values close to 1 (Table II).

An understanding of the reductions for the tetranuclear complex follows from the preceding discussion. The waves at  $-0.31$  and  $-1.10$  V vs. SSCE in the trinuclear complex are "split" into two components. The  $n$  value of the composite reductions at  $-0.22$  and  $-0.36$  V vs. SSCE was 2.0, indicating that each cyclic wave corresponds to a one-electron process. It follows from above that in the tetranuclear case the bridging ligand behaves as two subunits where the first and second reductions of one of the subunits are sensed by the other.

Finally it should be noted that the peak current for the first reduction of the mononuclear complex can be used to qualitatively substantiate previous assignments for voltammograms where  $n$  values were difficult to obtain.

**Reduction Potentials.** As pointed out previously, most reduction potentials for the  $\text{Ru}^{\text{III/II}}$  couples can be represented as composite waves consisting of two one-electron-transfer processes as shown by eq 4 and 5, 6 and 7, 8 and 9, and 10 and 11. The peak to peak separation between the oxidation and reduction waves is consistent with a two one-electron-transfer process as opposed to a two-electron-transfer step

(35) Johnson, E. C.; Callahan, R. W.; Eckberg, R. P.; Hatfield, W. E.; Meyer, T. J. *Inorg. Chem.* **1979**, *18*, 618.

(36) Powers, M. J.; Callahan, R. W.; Salmon, D. J.; Meyer, T. J. *Inorg. Chem.* **1976**, *15*, 894.

(37) Gagne, R. R.; Spiro, G. L. *J. Am. Chem. Soc.* **1980**, *102*, 1443.

(38) Richardson, D.; Taube, H. *Inorg. Chem.* **1981**, *20*, 1278.

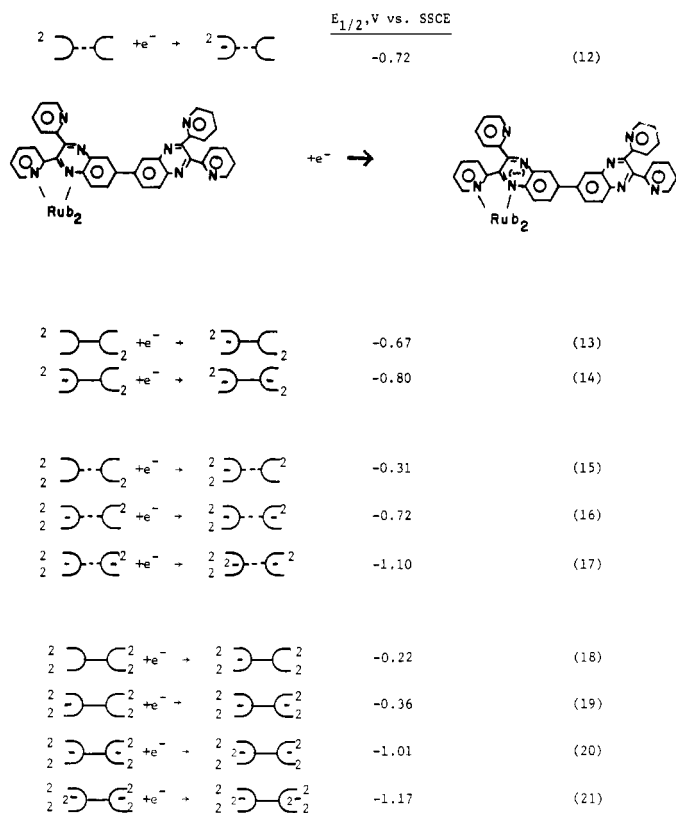
(39) (a) Creutz, C.; Taube, H. *J. Am. Chem. Soc.* **1973**, *95*, 1086. (b) Aoyagui, S. *J. Electroanal. Chem.* **1980**, *108*, 223.

(40) DeArmond, M. K.; Carlin, C. M. *Coord. Chem. Rev.* **1981**, *36*, 325.

where the peak to peak separation is expected to be 59/2 mV.<sup>28</sup>

|   | $E_{1/2}$ , V vs. SSCE |
|---|------------------------|
| $[3\text{---}3] + e^- \rightarrow [2\text{---}3]$ (4)                           | } 1.42                 |
| $[2\text{---}3] + e^- \rightarrow [2\text{---}2]$ (5)                           |                        |
| $[3,2\text{---}3] + e^- \rightarrow [2,2\text{---}3]$ or $[3,2\text{---}2]$ (6) | } 1.46                 |
| $[2,2\text{---}3]$ or $[3,2\text{---}2] + e^- \rightarrow [2,2\text{---}2]$ (7) |                        |
| $[3,3\text{---}3,3] + e^- \rightarrow [3,2\text{---}3,3]$ (8)                   | } 1.64                 |
| $[3,2\text{---}3,3] + e^- \rightarrow [3,2\text{---}3,2]$ (9)                   |                        |
| $[3,2\text{---}3,2] + e^- \rightarrow [3,2\text{---}2,2]$ (10)                  | } 1.46                 |
| $[3,2\text{---}2,2] + e^- \rightarrow [2,2\text{---}2,2]$ (11)                  |                        |

The dependence of the bridging ligand reduction potentials on the number of ruthenium complexes bound to it is illustrated in eq 12–21.<sup>41</sup> The solid line indicates cases where

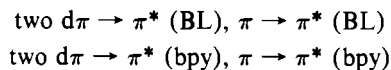


subunit–subunit interaction occurs between the bridging ligand component; the dashed line, cases where subunit–subunit interactions are not observed. The products in eq 13, 18, and 20 could be described as mixed valent and would fit in class II in the Robin and the Day<sup>42</sup> classification scheme.

**Ultraviolet–Visible Spectra.** The ultraviolet–visible spectra of the ligand-bridged complexes are dominated by a series of intense absorption bands (Table II). For complexes of the type  $[\text{Ru}(\text{bpy})_2\text{XL}]^+$ , very intense UV bands characteristically occur at  $\sim 290$  and  $\sim 240$  nm, which have been assigned to  $\pi \rightarrow \pi^*$  electronic transitions associated with the bipyridine ligands. There are also intense bands in the visible spectra assigned to  $d\pi\text{---}\pi^*$  transitions.<sup>24</sup> A number of different transitions are possible due to degeneracy of the  $d\pi$  energy

levels and different  $\pi^*$  energy levels on the ligands. These bands often overlap, and only a single maximum is observed along with a shoulder.<sup>24</sup>

The bridging ligand in the complexes reported here also contains a  $\pi$  system that appears to behave relatively independent of the  $\pi$  system of the remaining bipyridine ligands. Furthermore, electrochemical data imply that the  $\pi^*$  level lies lower in energy than that of the bipyridine ligands. The bridging ligand is also a better  $\pi$  acceptor than the bipyridine ligands, causing the  $d\pi$  level to lie somewhat lower in energy than for  $\text{Ru}(\text{bpy})_3^{2+}$ . Transitions for which absorption bands might be expected include



On the basis of electrochemical data and the arguments presented above, one would qualitatively predict the transitions to occur in the following energetic order:  $d\pi \rightarrow \pi^* (\text{BL}) < d\pi \rightarrow \pi^* (\text{bpy}) < \pi \rightarrow \pi^* (\text{BL}) < \pi \rightarrow \pi^* (\text{bpy})$ .

Thus for the mononuclear and binuclear complexes, the absorption at  $\sim 525$  nm corresponds to the  $d\pi \rightarrow \pi^* (\text{BL})$  absorption, the bands at  $\sim 420$  and  $380$  nm to the  $d\pi \rightarrow \pi^* (\text{bpy})$  transitions, and the absorptions at  $\sim 284$  and  $\sim 248$  nm to the  $\pi \rightarrow \pi^* (\text{bpy})$  transitions. The  $\pi \rightarrow \pi^* (\text{BL})$  absorptions are apparently masked by the very intense  $\pi \rightarrow \pi^* (\text{bpy})$  bands.

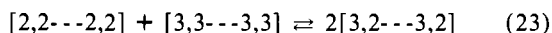
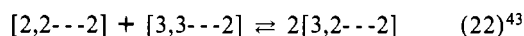
The trinuclear complex contains two subunits, one which is characteristic of a binuclear system where metal–metal interaction occurs and a second subunit which behaves as a mononuclear complex. It has previously been shown that the  $d\pi \rightarrow \pi^* (\text{BL})$  transition is strongly affected by a remote metal since the transitions are directed along the metal–metal axis.<sup>39a</sup> For such cases, a red shift for the  $d\pi \rightarrow \pi^* (\text{BL})$  transition has previously been observed.<sup>24,39a</sup> Apparently stabilization of the  $\pi^*$  excited state of the bridging ligand results in a lower energy due to the remote positive charge. For the trinuclear complex, then, a new  $d\pi \rightarrow \pi^* (\text{BL})$  band is observed at 606 nm and a slight red shift is noted in the 520 nm band, presumably due to band overlap.

For the tetranuclear complex, the  $d\pi \rightarrow \pi^* (\text{BL})$  transition at  $\sim 525$  nm nearly disappears. One might expect that the  $\pi \rightarrow \pi^* (\text{BL})$  bands would also shift in the same direction as the  $d\pi \rightarrow \pi^*$  transitions. These, however, remain hidden under intense  $\pi \rightarrow \pi^* (\text{bpy})$  transitions, and no conclusions can be reached.

An interesting comparison can be made between energy changes observed spectrally and those found electrochemically. The difference between  $\lambda_{\text{max}}$  values for the low-energy bands in the mononuclear and trinuclear complexes is  $3.0 \times 10^3 \text{ cm}^{-1}$  or about 0.36 eV. The reduction potentials for the  $\text{Ru}^{2+/+}$  couples of the compounds change by 0.41 V, indicating that both spectral and potential energies decrease by similar amounts, lending additional evidence to the supposition that the  $\pi^*$  level of the bridging ligand is the lowest excited state.

There is an increase in the reduction potential of 0.07 V for the  $\text{Ru}^{3+/2+}$  couples upon forming  $[2,2\text{---}2]$  or  $[2,2\text{---}2,2]$ . This change is opposed to decreasing the energy gap between the  $d\pi$  and  $\pi^*$  energy levels. The increase in potential results from an increase in the charge of the molecule. Since the  $\pi^*$  (BL) orbital is much closer to the center of positive charge, it is most strongly affected and lowered in energy. This facilitates  $d\pi \rightarrow \pi^*$  back-bonding and hence lowers the energy of the  $d\pi$  levels.

**Mixed-Valent Species.** The comproportionation constants for reactions 22 and 23 were calculated by using the free



(41) The fact that reductions of the complexes are ligand centered (rather than metal centered as oxidations) gives rise to redox behavior of a second type. This is illustrated by using the notation in eq 12–21. A structure formula is given for eq 12. As pointed out in the text, the reductions correspond to addition of electrons to the  $\pi^*$  levels of the bridging ligand: Rillema, D. P.; Mack, K. B., submitted for publication.

(42) Robin, M. B.; Day, P. *Adv. Inorg. Chem. Radiochem.* **1967**, *10*, 247.



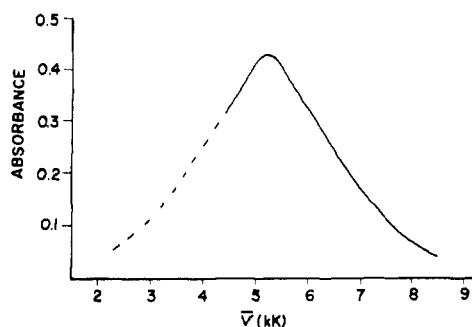


**Figure 6.** Near-infrared spectrum of  $[\text{Ru}(\text{bpy})_2]_4\text{BL}^{10+}$  in acetonitrile at  $20 \pm 1$  °C. The low-energy side was traced in, ---, with the assumption of Gaussian symmetry about the center of the band.

energy relationship  $\Delta E_{1/2} = 0.0591 \log K_{\text{com}}$ . The values were  $8 \times 10^2$  for reaction 22 and  $1 \times 10^3$  for reaction 23. These values are similar to those found for bidentate bridging ligand compounds such as  $[\text{Ru}(\text{bpy})_2]_2\text{BL}^{5+}$  ( $1.1 \times 10^2$ ),<sup>13</sup> where BL = 2,2'-bipyrimidine, and for monodentate bridging ligand pyrazine (pyr) complexes such as  $[\text{Ru}(\text{bpy})_2\text{Cl}]_2\text{pyr}^{3+}$  ( $1 \times 10^2$ ).<sup>32</sup>

The mixed-valent forms of the complexes in eq 22 and 23 were generated electrochemically in acetonitrile containing 0.1 M TEAP as supporting electrolyte. Near-infrared spectra were obtained by scanning from 2200 nm to higher energy. Solvent interference at longer wavelengths was appreciable. Thus, the low-energy side of the spectrum in Figure 6 was traced in by assuming a band shape similar to that of the high-energy component. The bands are broad and are located at  $\approx 1900$  nm, which is comparable in energy to that of some mixed-valent forms of ferrocene compounds.<sup>44</sup> Spectra of this type have been attributed to intervalent electron transfer (IT).<sup>24,39a,44</sup>

The bandwidth at half-height,  $\bar{\nu}_{1/2}$ , was determined by assuming that the band was symmetrical around  $\bar{\nu}_{\text{max}}$ .  $\bar{\nu}_{1/2}$  is defined as the value of  $\Delta\nu$  where  $A_{\bar{\nu}_{1/2}}/A_{\text{max}} = 1/2$ <sup>45</sup> holds;  $A_{\bar{\nu}}$  and  $A_{\text{max}}$  are absorbances at  $\bar{\nu}$  and  $\bar{\nu}_{\text{max}}$ , respectively. The experimental values of  $\bar{\nu}_{1/2}$  for both trinuclear and tetranuclear mixed-valent species were  $(3.3 \pm 0.1) \times 10^3 \text{ cm}^{-1}$ , and the values calculated by using the equation  $\bar{\nu}_{\text{max}} - \bar{\nu}_0 = \bar{\nu}_{1/2}^2/2.31$  were  $3.4 \times 10^3 \text{ cm}^{-1}$ . The value for  $\bar{\nu}_0$ , where  $\bar{\nu}_0$  is the ground-state internal energy difference following thermal electron transfer, was determined from the equation  $\bar{\nu}_0 (\text{cm}^{-1} \times 10^3) = 8.08[E'_{1/2} - E_{1/2}(1)]$ ,<sup>36</sup> where  $E'_{1/2}$  was taken from Table I as the potential for oxidation of the mononuclear complex (1.41 V) and  $E_{1/2}(1)$  was taken as the potential for the first oxidation of the tetranuclear complex (1.46 V).

Equation 24 can be used to obtain a measure of ground-state

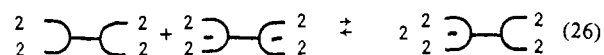
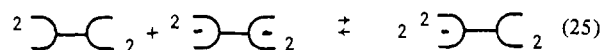
$$\alpha^2 = \frac{1}{g} \frac{(4.2 \times 10^{-4})\epsilon_{\text{max}} \bar{\nu}_{1/2}}{\bar{\nu}_{\text{max}} d^2} \quad (24)$$

delocalization ( $\alpha^2$ ) in mixed-valent complexes, where  $\epsilon_{\text{max}}$  is the molar extinction coefficient at  $\bar{\nu}_{\text{max}}$ ,  $d$  is the distance between metal centers ( $6.8 \text{ \AA}$ ),<sup>46</sup> and  $g$  is the degeneracy of the

excited state. For the trinuclear mixed-valent species  $g = 1$ , whereas for the tetranuclear case  $g = 2$ . The  $\alpha^2$  values obtained were  $5.3 \times 10^{-3}$  and  $3.0 \times 10^{-3}$  for the trinuclear and tetranuclear complexes, respectively. These values are comparable to those of other complexes described as mixed valent ( $\alpha^2 = 2.0 \times 10^{-3}$ <sup>24</sup> for  $[\text{Ru}(\text{bpy})_2\text{Cl}]\text{pyr}^{3+}$  and ranges from  $2.4 \times 10^{-3}$  to  $9 \times 10^{-3}$  for mixed-valent ferrocene<sup>47</sup> derivatives).

The activation energies  $E_{\text{th}}$  ( $E_{\text{th}} \approx E_{\text{op}}/4$ , where  $E_{\text{op}}$  is the energy at  $\bar{\nu}_{\text{max}}$ ) for thermal electron transfer are  $\sim 3.8$  kcal/mol, and the rates of intrametal electron transfer  $k_{\text{et}}$  ( $k_{\text{et}} = (k_{\text{B}}T/h)e^{-E_{\text{th}}/RT}$ ) are  $\sim 1 \times 10^{10} \text{ s}^{-1}$  for both the trinuclear and tetranuclear mixed-valent complexes. If the effects of delocalization are included in the estimates,  $E_{\text{th}} \approx (E_{\text{op}}/4) - H_{12}$ , where  $H_{12}$  arises through resonance interaction between the two metal sites,<sup>48,49,50</sup> gives  $E_{\text{th}} \approx 2.5$  kcal/mol and  $k_{\text{et}} \approx 8 \times 10^{10} \text{ s}^{-1}$ . The thermal rate constants are approximately tenfold greater than observed for some pyrazine-bridged complexes.<sup>16,17</sup> The difference is reflected in the lower activation barriers ( $\approx 2$  kcal), giving rise to more facile intrametal electron exchange.

The comproportionation constants for reactions 25 and 26



were calculated to both be  $\approx 1.6 \times 10^2$  and suggest that the products in eq 25 and 26 should be mixed valent. The products were generated electrochemically in acetonitrile containing 0.1 M TEAP as the supporting electrolyte. We were unable to observe a near-infrared band characteristic of the mixed-valent forms. It may be that the bands lie at lower energy ( $< 2300$  nm) or the molar absorption coefficients are very low for the species. Nevertheless, the important implications are that  $\sim 8\%$  of the singly reduced complex is in the doubly reduced form. Thus, such compounds could be photochemically or electrochemically reduced by one electron and still function as a two-electron-transfer agent and, thus, for example, catalyze the reduction of water to hydrogen.<sup>48</sup> In addition, the [2--2] compound contains both a weakly luminescing chromophore ( $\Phi \approx 10^{-6}$ ) and nitrogen donor atoms, which can act as sites for proton reduction.

**Acknowledgments** are made to the Petroleum Research Fund, administered by the American Chemical Society, to the Foundation at The University of North Carolina at Charlotte, to the National Science Foundation for funds to purchase the luminescence spectrophotometer, and to the North Carolina Board of Science and Technology for funds to purchase a coulometer.

**Registry No.** BL, 81294-31-7;  $[\text{Ru}(\text{bpy})_2]\text{BL}(\text{PF}_6)_2$ , 81316-17-8;  $[\text{Ru}(\text{bpy})_2]_2\text{BL}(\text{PF}_6)_4$ , 81316-19-0;  $[\text{Ru}(\text{bpy})_2]_3\text{BL}(\text{PF}_6)_6$ , 81316-21-4;  $[\text{Ru}(\text{bpy})_2]_4\text{BL}(\text{PF}_6)_8$ , 81316-23-6;  $[\text{Ru}(\text{bpy})_2\text{Cl}]_2$ , 19542-80-4; 3,3'-diaminobenzidine, 91-95-2; 2,2'-pyridil, 492-73-9.

(43) For eq 22, the potential of  $[3,3\text{---}2] + e^- \rightarrow [3,2\text{---}2]$  is taken to be equal to that of  $[3,3\text{---}3] + e^- \rightarrow [3,2\text{---}3]$ .

(44) Brown, G. M.; Meyer, T. J.; Cowan, D. O.; LeVanda, G.; Kaufman, F.; Roling, P. V.; Rausch, M. D. *Inorg. Chem.*, **1975**, *14*, 506.

(45) Hush, N. S. *Prog. Inorg. Chem.* **1967**, *8*, 391. Hush, N. S. *Electrochim. Acta* **1968**, *1905*.

(46) The distance was determined from metal center to metal center directly through space on the basis of a crystal structure of the mononuclear portion of the molecule: Levy, H.; Jones, D. S.; Rillema, D. P., unpublished observations.

(47) Powers, M. J.; Meyer, T. J. *J. Am. Chem. Soc.* **1978**, *100*, 4393.

(48) Callahan, R. W.; Keene, F. R.; Meyer, T. J.; Salmon, D. J. *J. Am. Chem. Soc.* **1977**, *99*, 1064.

(49) Creutz, C.; Kroger, P.; Matsubara, T.; Netzel, T. L.; Sutin, N. *J. Am. Chem. Soc.* **1979**, *101*, 5442.

(50) Abruna, H. D.; Teng, A. Y.; Samuels, G. J.; Meyer, T. J. *J. Am. Chem. Soc.* **1980**, *102*, 6746.